

Estimation of CO₂ emission strength from a mega-sized city using satellite and in situ observation data

R. Imasu⁽¹⁾ Y. Arai⁽¹⁾, H. Kondo⁽²⁾, Y. Niwa⁽³⁾, Y. Sawa⁽³⁾, H. Matsueda⁽³⁾
T. Machida⁽⁴⁾, Y. Yoshida⁽⁴⁾, T. Yokota⁽⁴⁾, Y. Matsumi⁽⁵⁾ and N. Saitoh⁽⁶⁾

(1) Atmosphere and Ocean Research Institute (AORI), The University of Tokyo

(2) National Institute of Advanced Industrial Science and Technology (AIST)

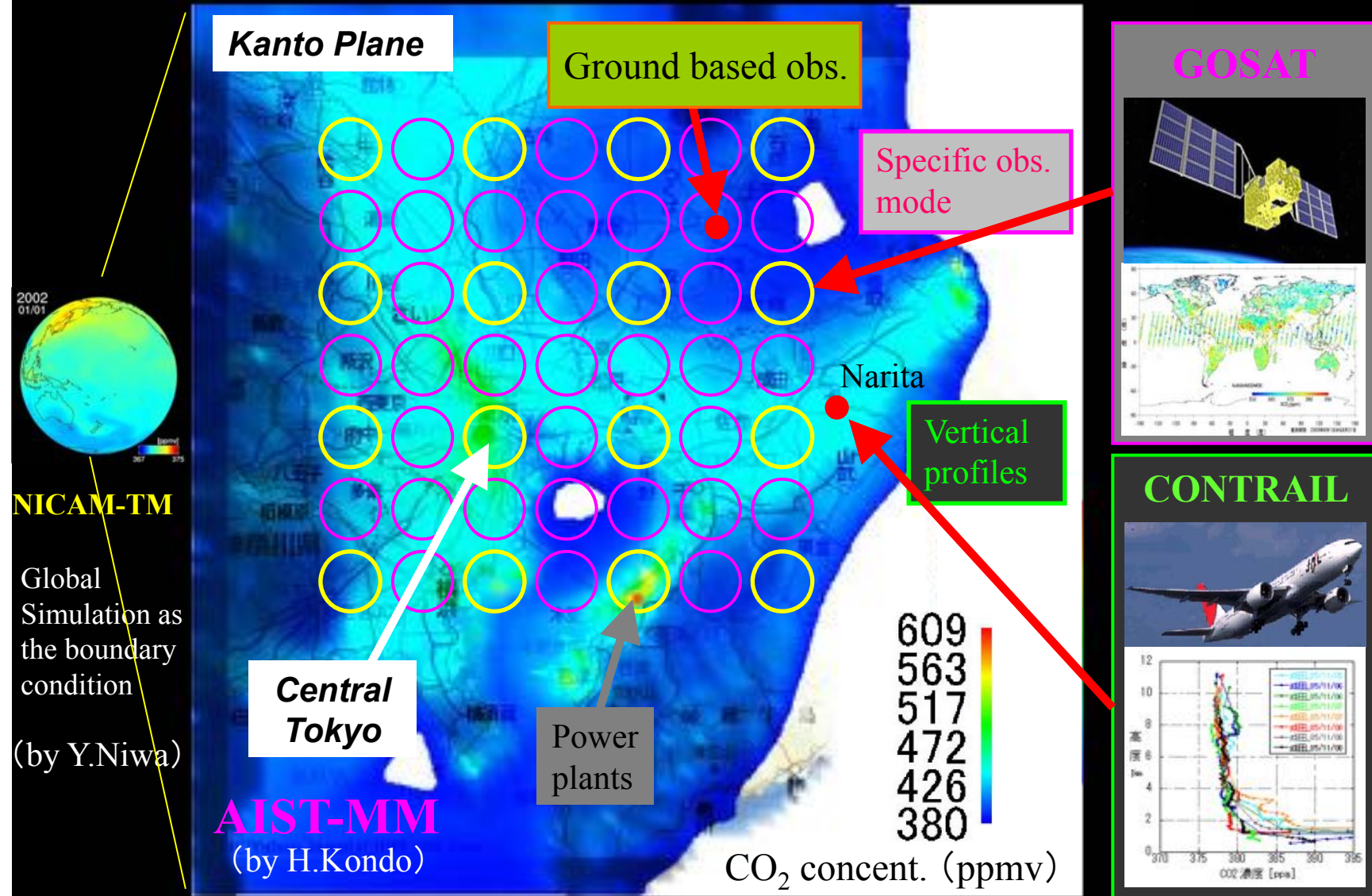
(3) Meteorological Research Institute (MRI), Japan Meteorological Agency (JMA)

(4) National Institute for Environmental Studies (NIES)

(5) Solar-Terrestrial Environment Laboratory, Nagoya University

(6) Center for Environmental Remote Sensing (CEReS), Chiba University

CO_2 Data assimilation using AIST-MM and NICAM-TM



Objective : Developing CO_2 Data assimilation system for assessing urban CO_2 emissions

Observational data

【Monitoring by local government】 《ground based, continuous: hourly》

Center for Environmental Science in Saitama (WDCGG) : 2000~

Tokyo Metropolitan Res. Inst. for Environmental Protection ・・・ 2000～

Ibaraki prefectural government 2000(2004)~

Kanagawa prefecture, Chiba prefecture ···?

【CONTRAIL】《Vertical profiles, upper tropospheric concentration》

Data provided by Dr. Machida (NIES), Dr. Matsueda and Sawa (MRI/JMA)

※Vertical profiles around Narita airport (Chiba pref.)

(Machida et al., doi:10.1175/2008JTECHA1082.1, 2008)

【GOSAT】《SWIR:XCO₂, TIR: upper tropospheric concentrations》

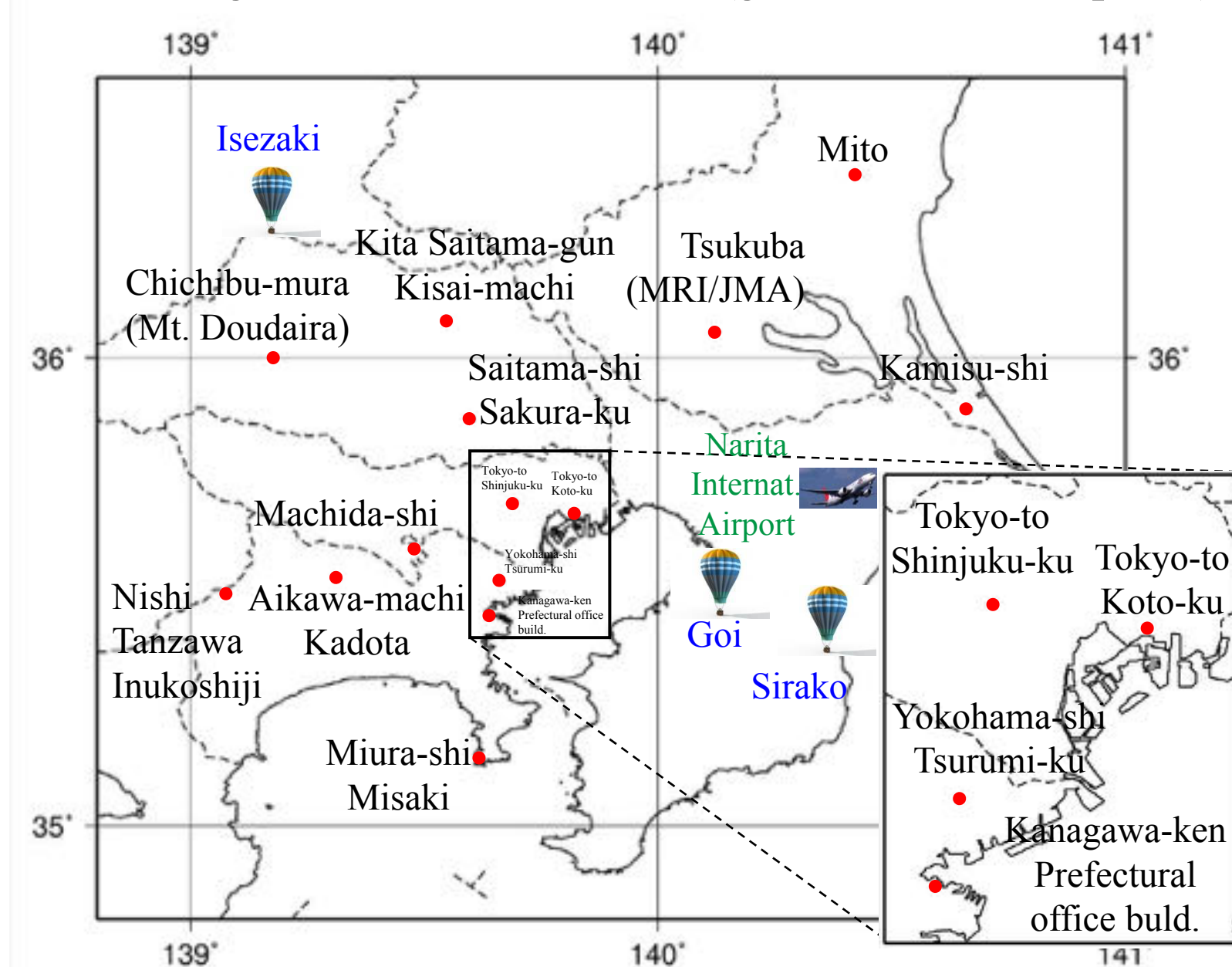
Targeting mode observations conducted GOSAT science team

1 path/6days, simultaneous 16(14) points over the Kanto plain

2 modes (validation point mode, mesh mode)

2010.11 ~ present

Location of ground observation sites (ground, sonde, airplane)



Transport model (forward calculation, inverse analysis)

【NICAM-TM】 《Global scale model based on GCM》

- Originally developed by Dr. Niwa (AORI/Univ. Tokyo, present affil. MRI/JMA)
(Niwa, Y., et al., J. Meteo. Soc. Jpn., 89, 255-, 2011)
- Nudging of meteorological data: NCEP
- Fossil fuel emission, Surface flux based on a biosphere mode (CASA)
Biomass burning (GFED3),
Ocean uptake (Takahashi, 2008)

【AIST-MM】 《Regional scale model》

- Originally developed by Dr. Kondo (AIST)
(Kondo, H., J. Meteo. Soc. Jpn. 68, 419-, 1990,
Kannari, A. et al., *Atmos. Env.*, 41, 3428-, 2007)
- Nudging of meteorological data: GPV-MSM (forecast)
- Anthropogenic emissions (Kannari, 2000), uptake by biosphere

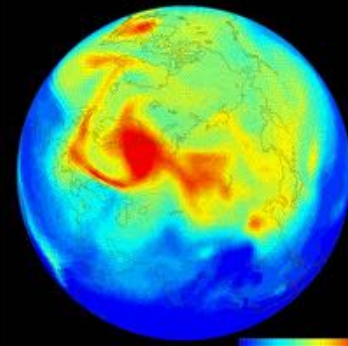
※ Inversion analysis: Synthesis inversion

Down scaling of transport calculation model

Horizontal resolution=2km (Max. 1km)

Global → regional

NICAM-TM



By Y. Niwa

DATA: CO2 CONC., DATE: 12202NOV2010

Wind direction: NW

AIST-MM

DATA: CO2 CONC., DATE: 12220NOV2010

Wind direction: SE

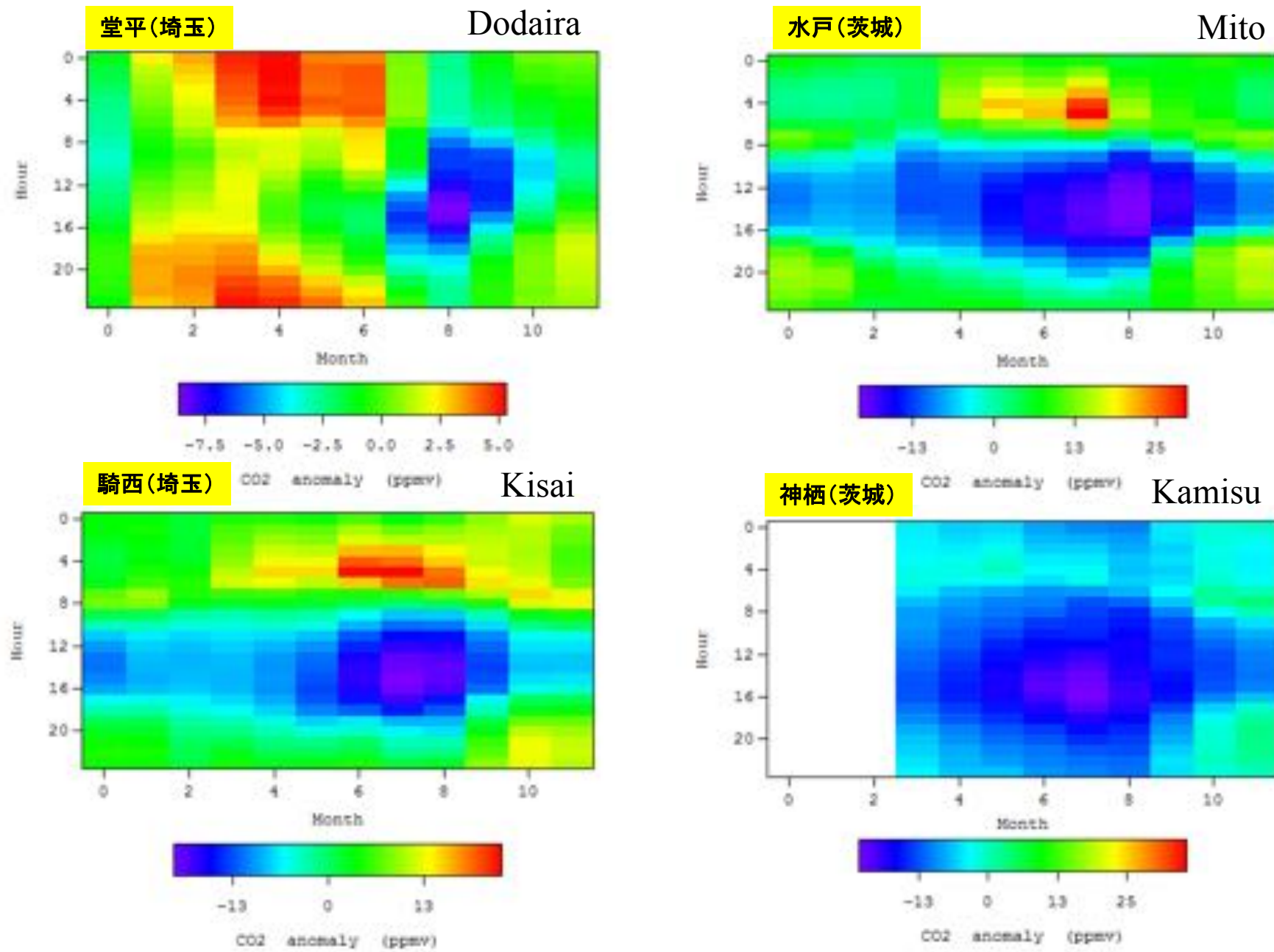
DATA: CO2 CONC., DATE: 12202NOV2010

火力発電所
Power plant

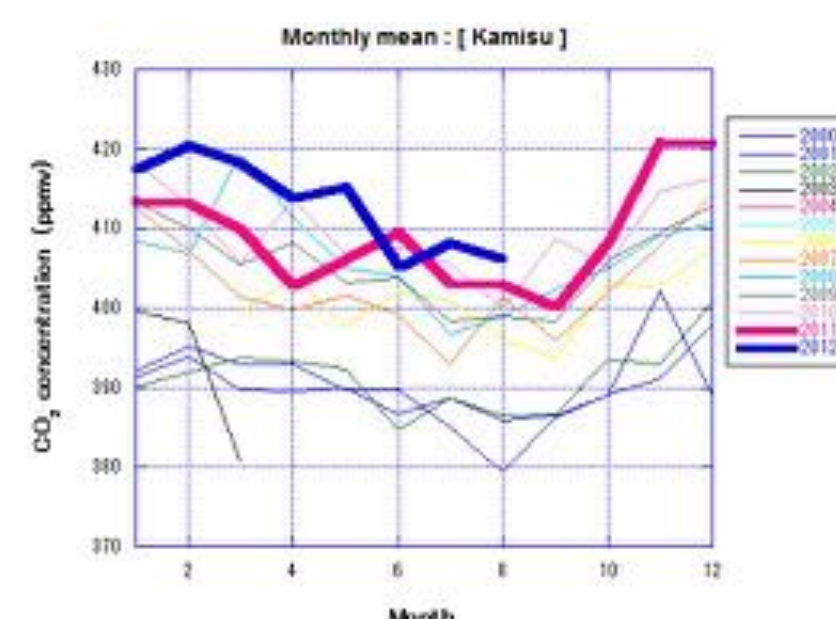
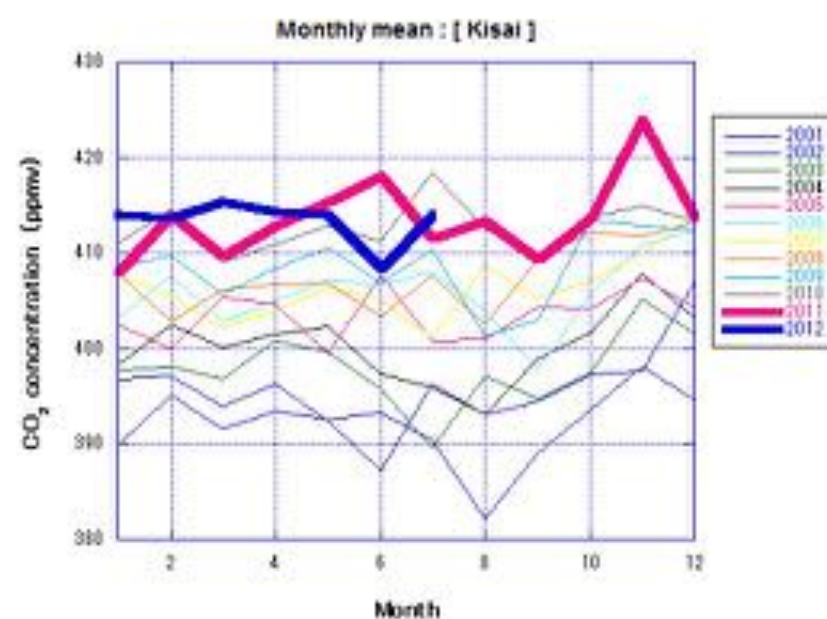
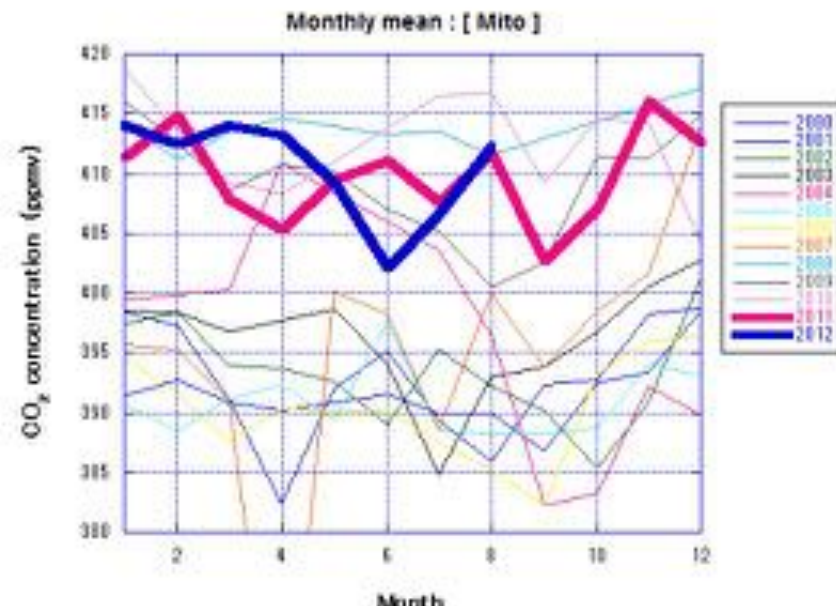
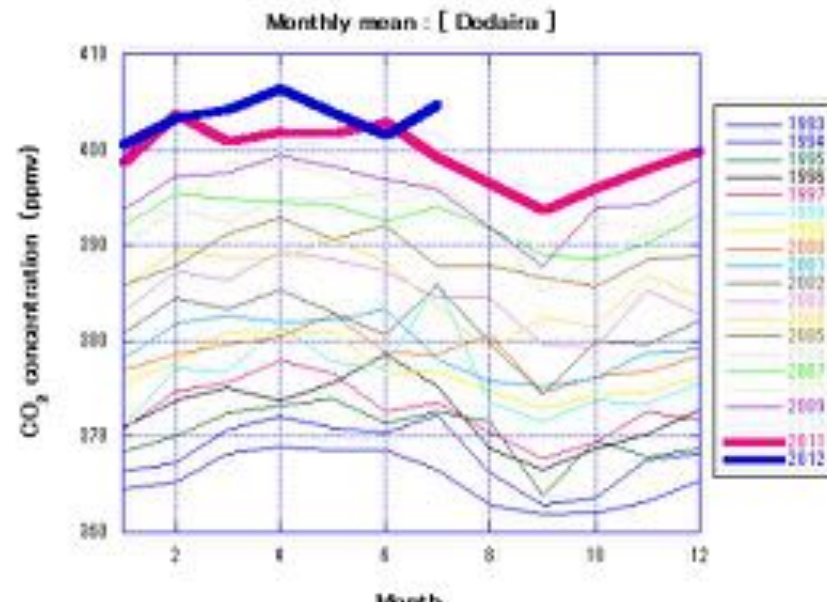
DATA: CO2 CONC., DATE: 12220NOV2010

CO2 concentration [ppm]

Seasonal variation of CO₂ diurnal cycle at the surface

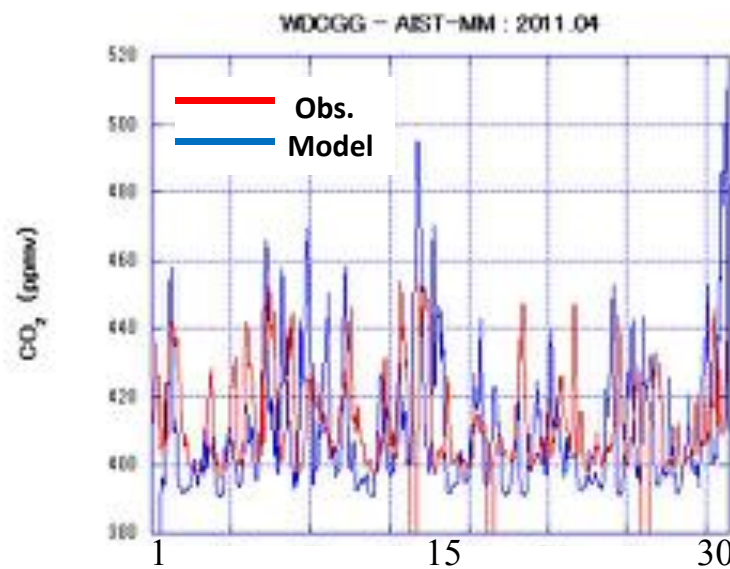


Changes in CO₂ concentrations detected after the Tohoku-Pacific Ocean Earthquake

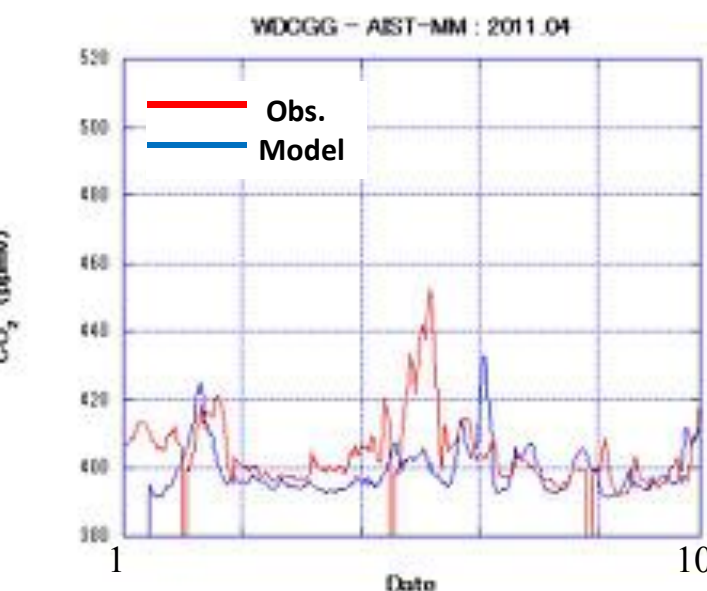
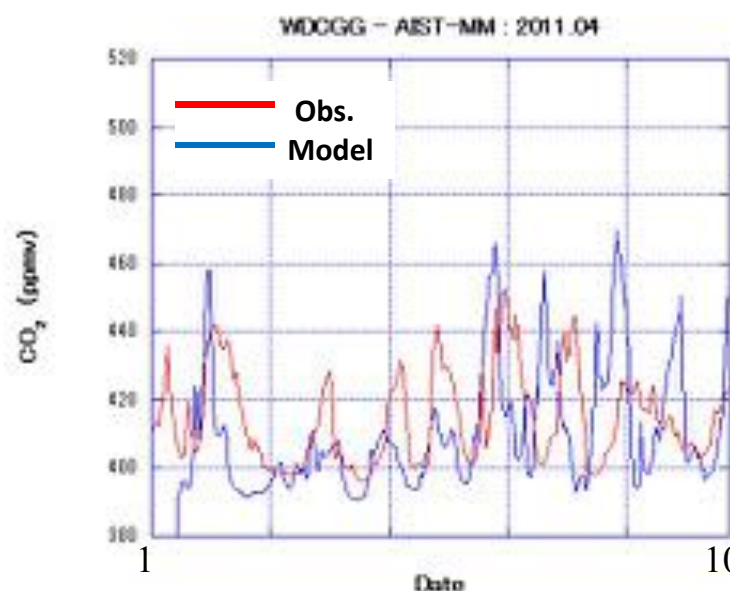
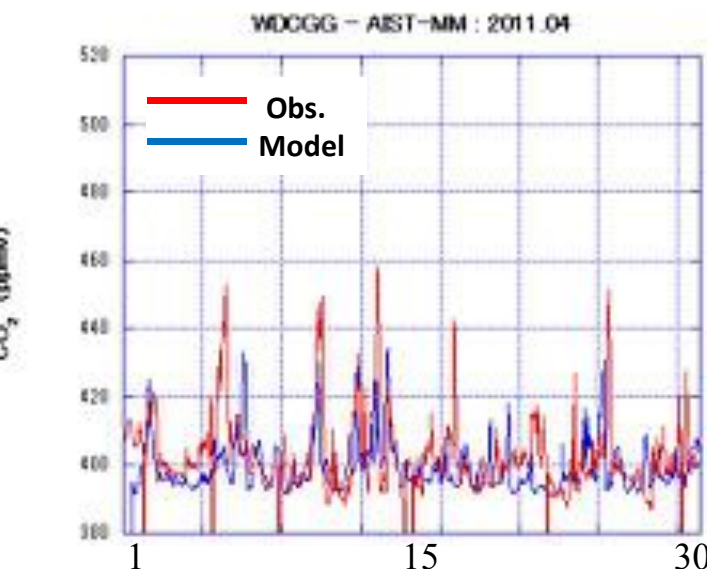


Comparison between observation and model calculation

Kisai (Saitama)



Kamis (Ibaraki)



CO₂: GOSATによる関東集中観測開始

注)衛星運用はJAXA, NIESが実施
本研究課題では観測要求とデータ
解析を実施

- CO₂、O₃、CH₄観測点の強化とデータ蓄積
- GOSATのメインセンサー“TANSO-FTS”の特定点観測モード利用
- 4点×4点(計16点)の集中観測を2010年11月を開始
- すべての検証点を含むタイプ1と、関東地域をほぼ等間隔でカバーするタイプ2を設定し、それぞれ12日おき、2つのモードを併せて、6日ごとに集中観測を実施

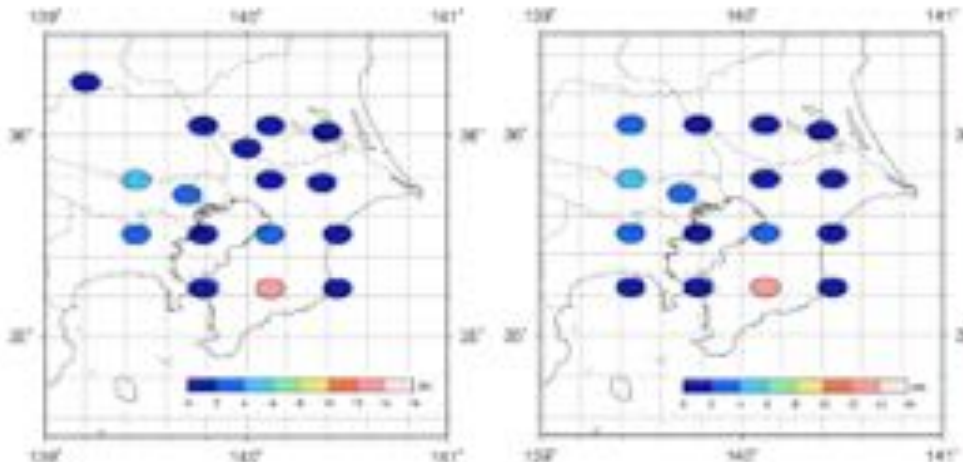


図1 GOSAT集中観測における2つの観測パターンにおける観測地点。左がタイプ1で全検証点を含む。右がタイプ2でほぼメッシュ点における観測。色は視野内の標高の分散値。

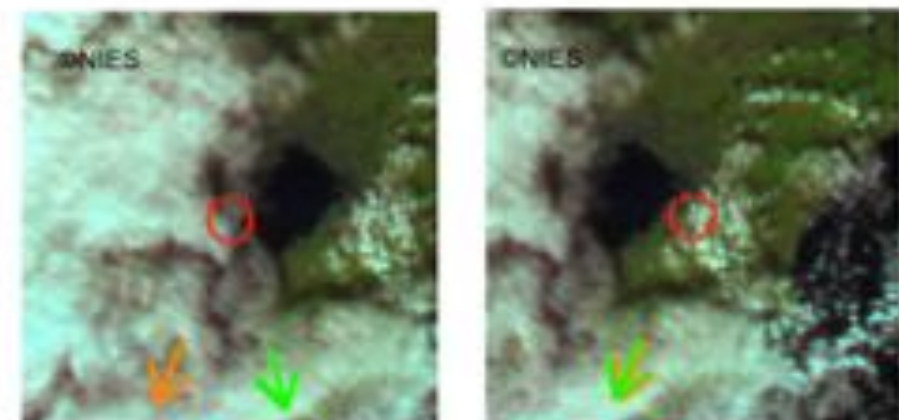


図2 GOSAT集中観測時のTANSO-CAI画像の例。観測日は2010年12月2日。この日はあいにく曇り点が多くかった。
(データ:国立環境研究所提供)

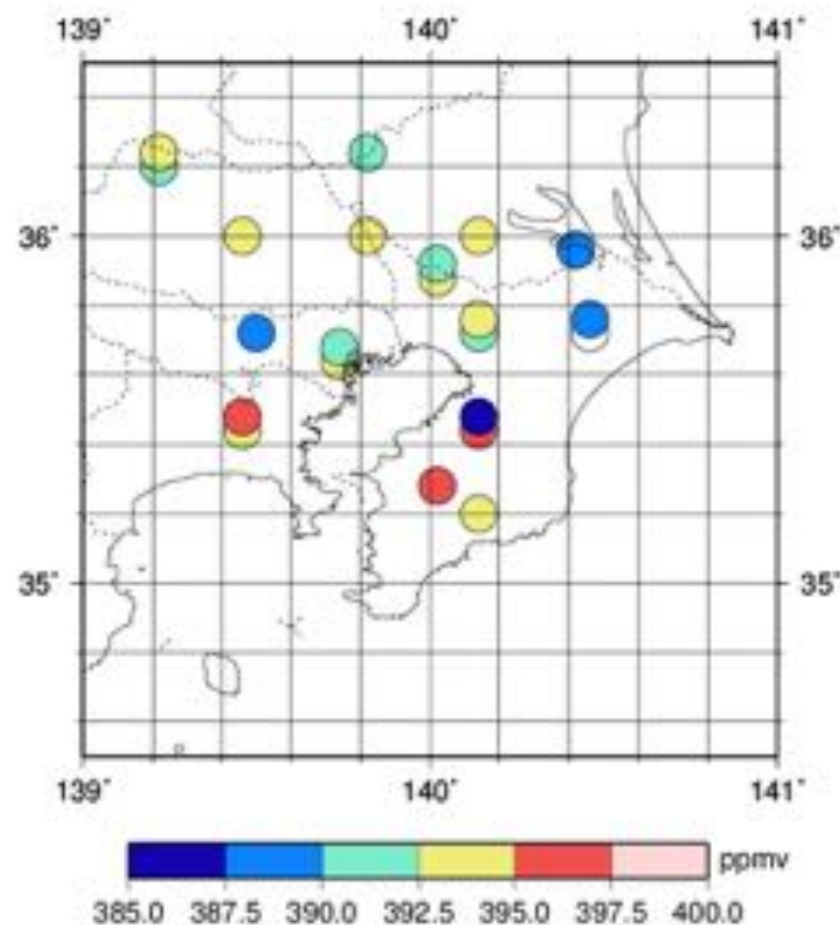
	Obs. point No.	1	2	3	4	5	6	7	8	9	10	11	12	13	14	15	16
Type2	2010/11/02																
	2010/11/14																
	2010/11/26																
Type1	2010/11/08																
	2010/11/20																

2010年11月の観測結果のまとめ。“斜線”, “×”, “○”, “◎”はそれぞれ、“欠測”, “曇天”, “晴天、ただしL2データ未処理”, “L2データまで処理完了”である。

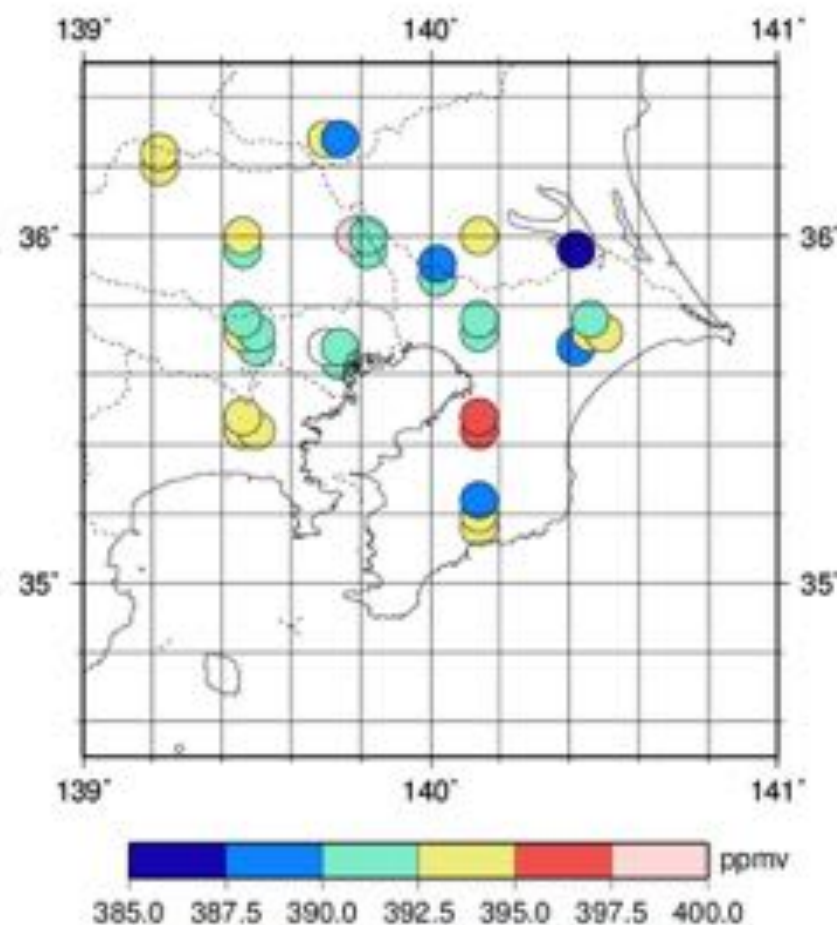
XCO₂ observed by GOSAT TANSO-FTS (SWIR) over the Kanto Plain

2010.11 ~ 2012.11

May~September

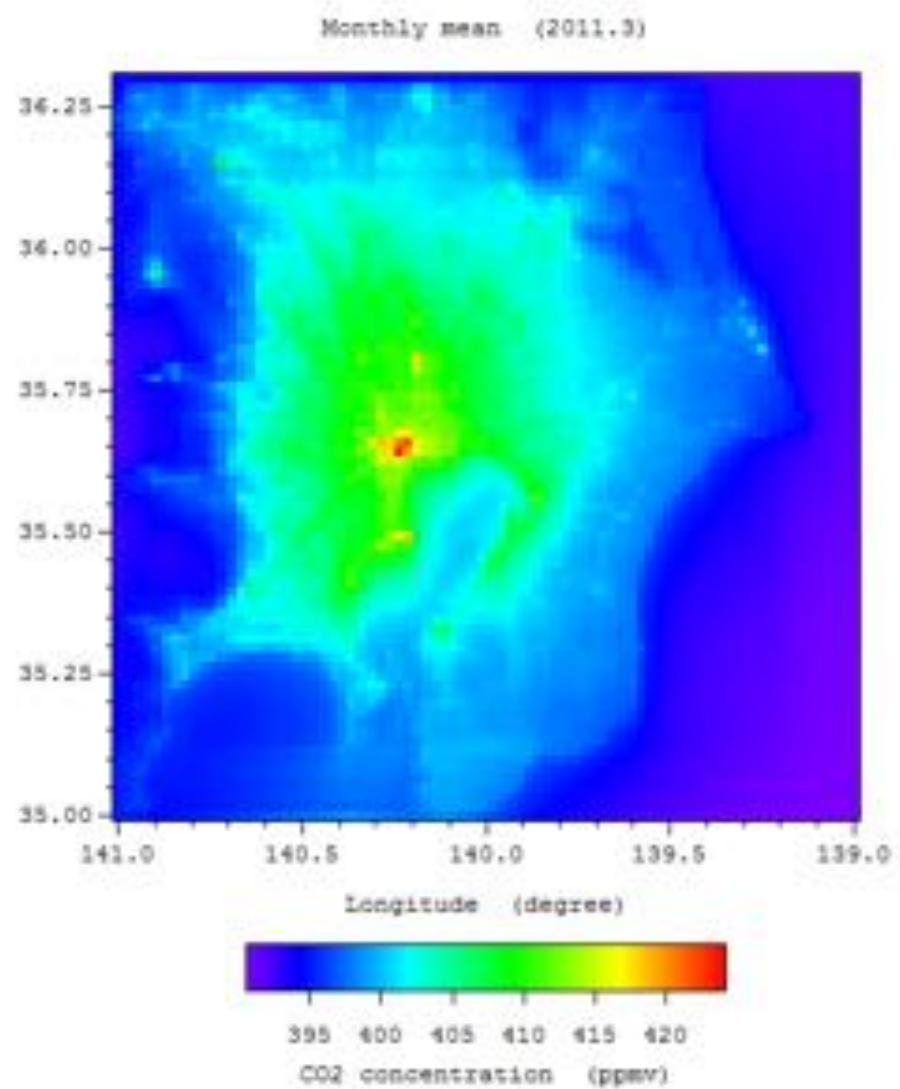
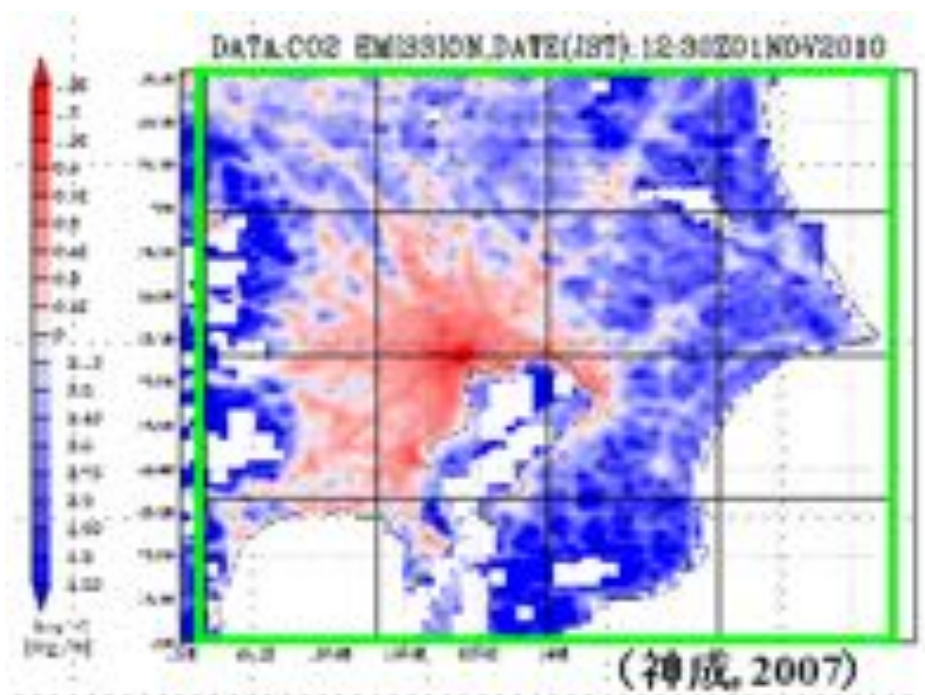


October~April

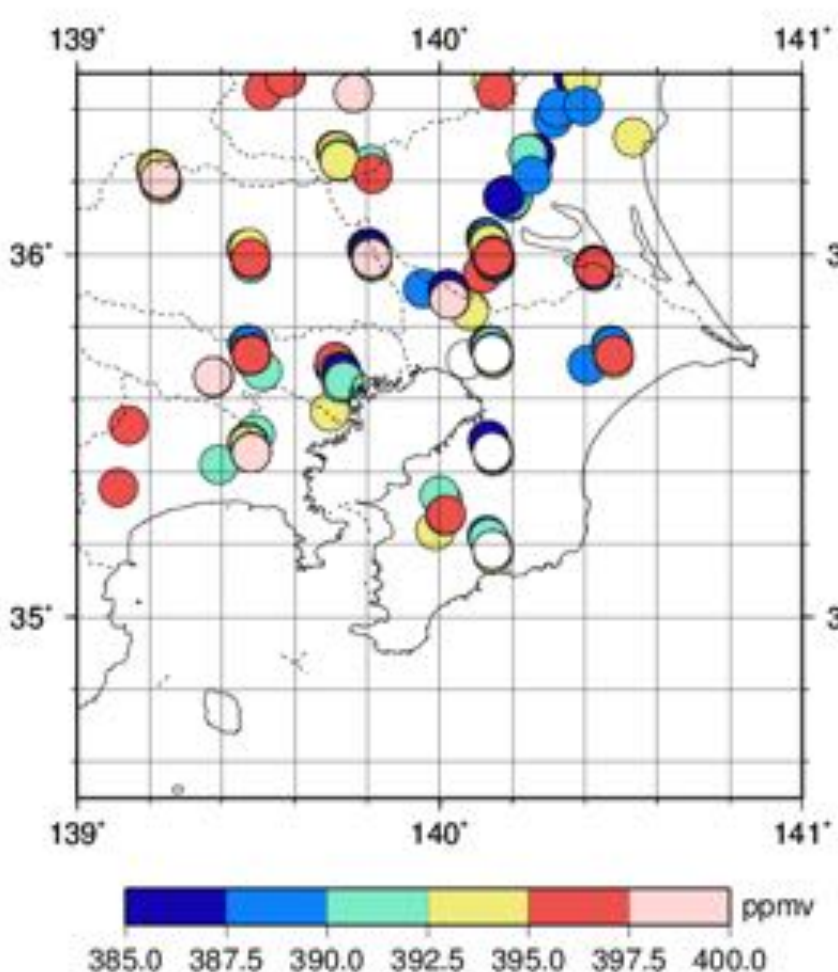


Mothly mean CO₂ surface concentration
calculated by AIST-MM for 2011.3

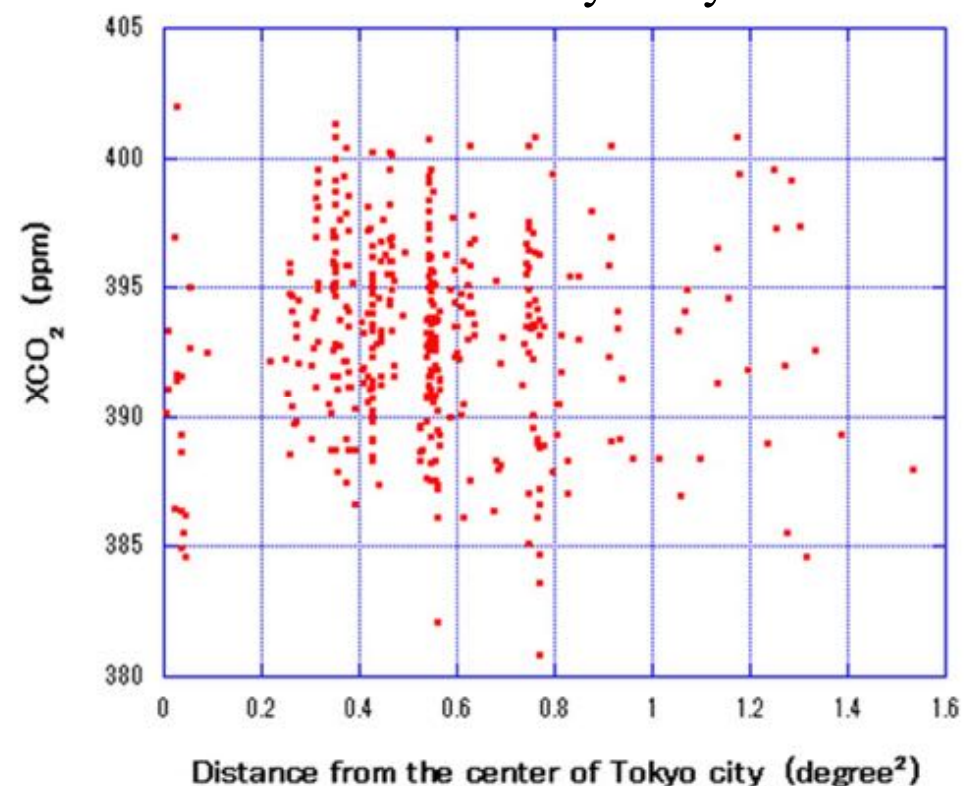
CO₂ Emission inventory data



GOSAT-SWIR - XCO₂
2010.11 ~ 2013.3

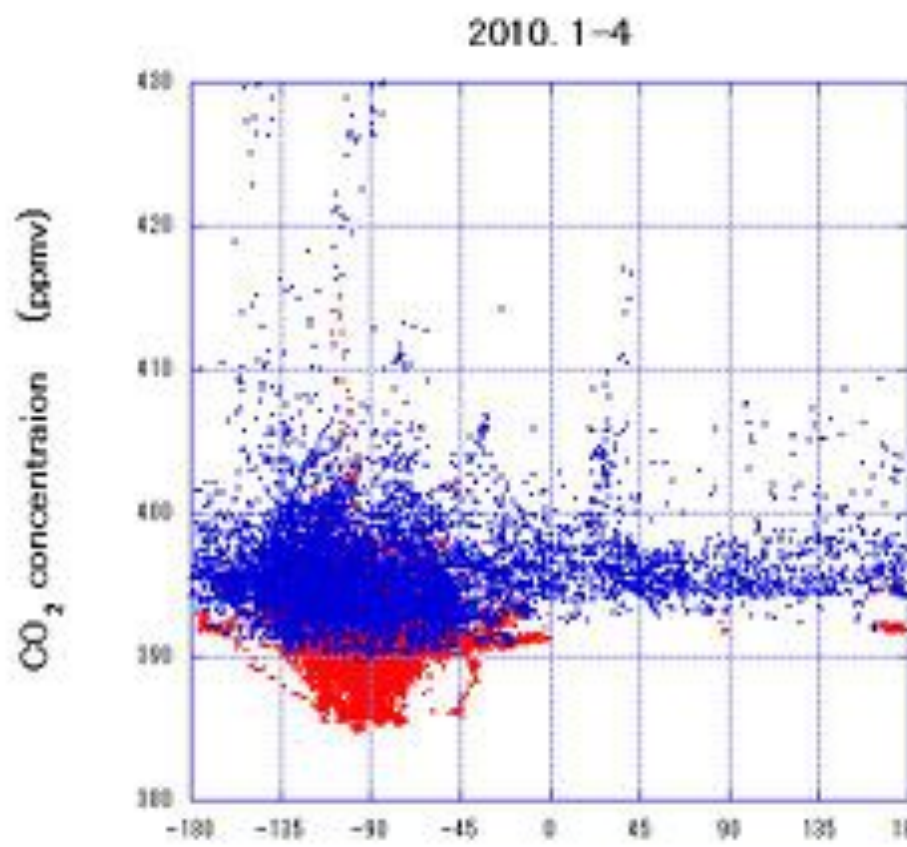


GOSAT-SWIR-XCO₂ as a function
of distance of obs. point from the center
of the Tokyo city



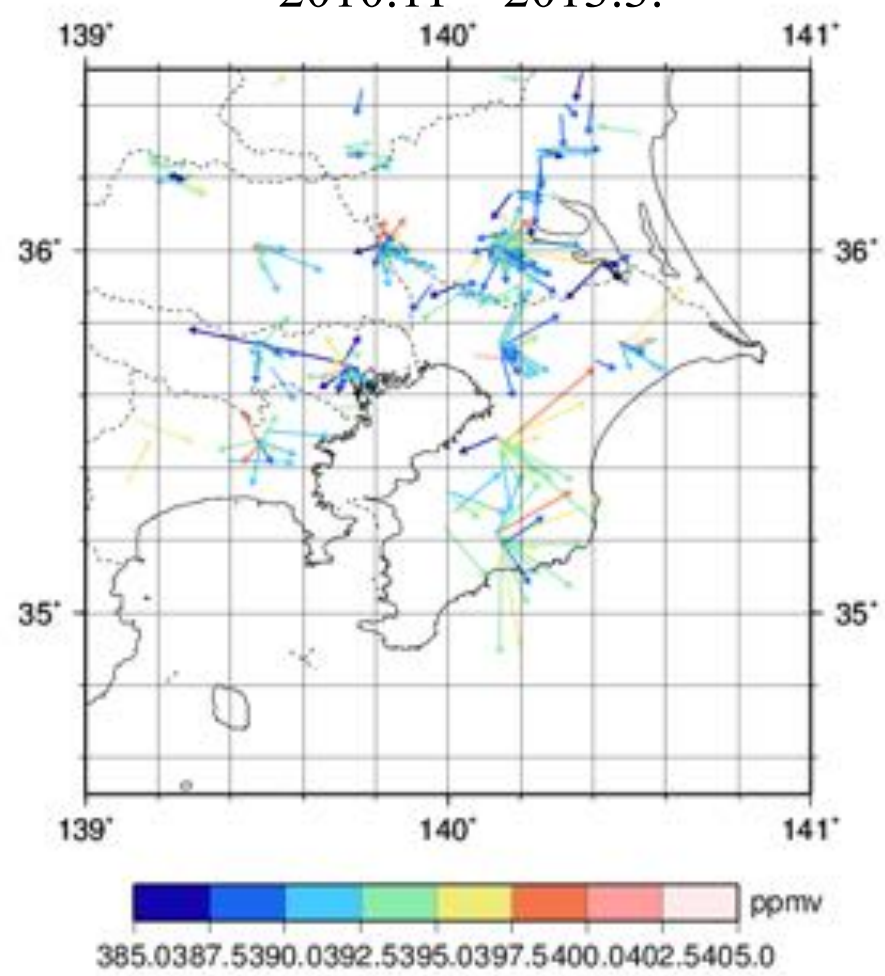
Relationship between XCO₂ and wind direction/speed

CONTRAIL 2009

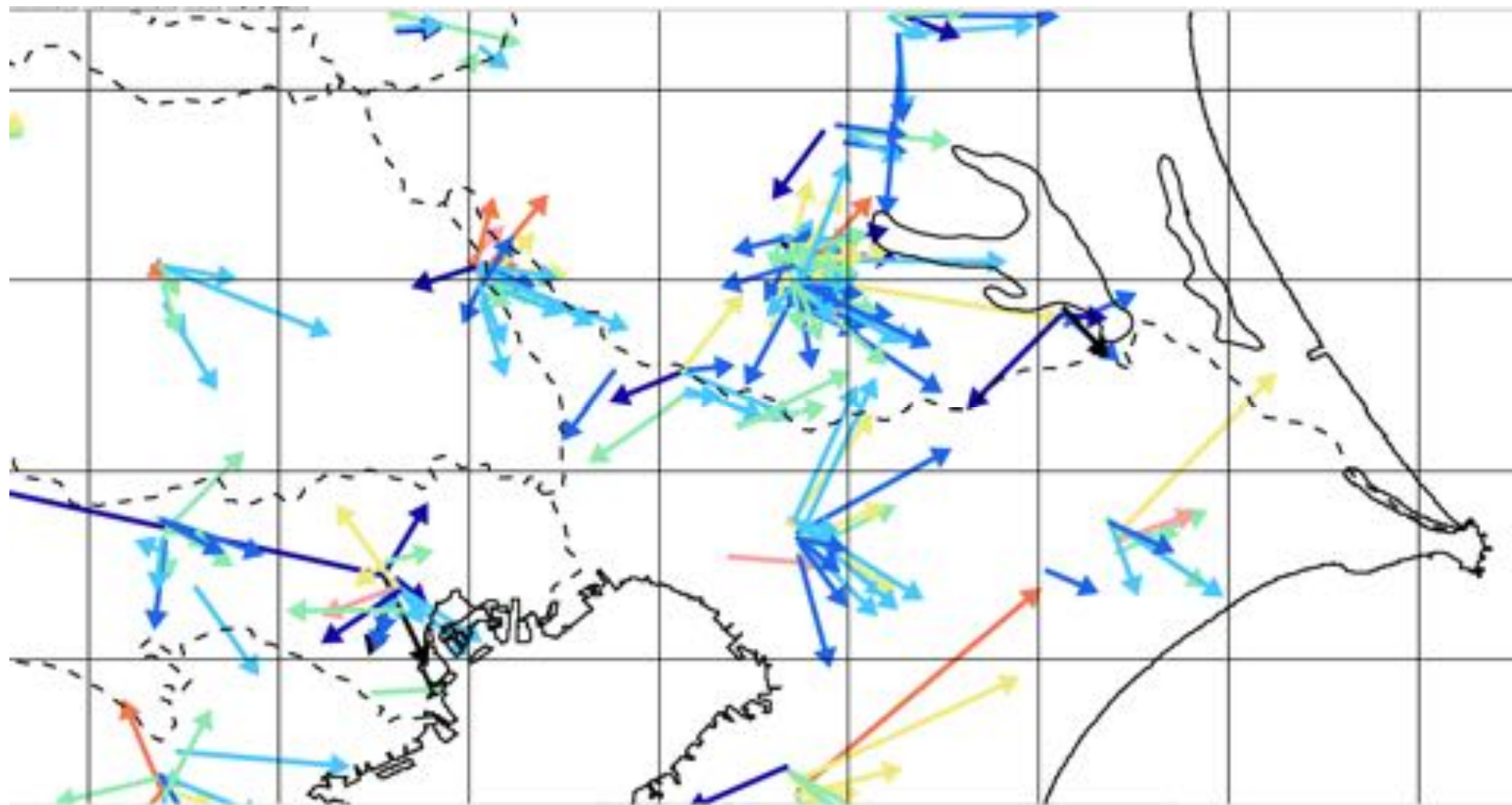


(Data : T. Machida)

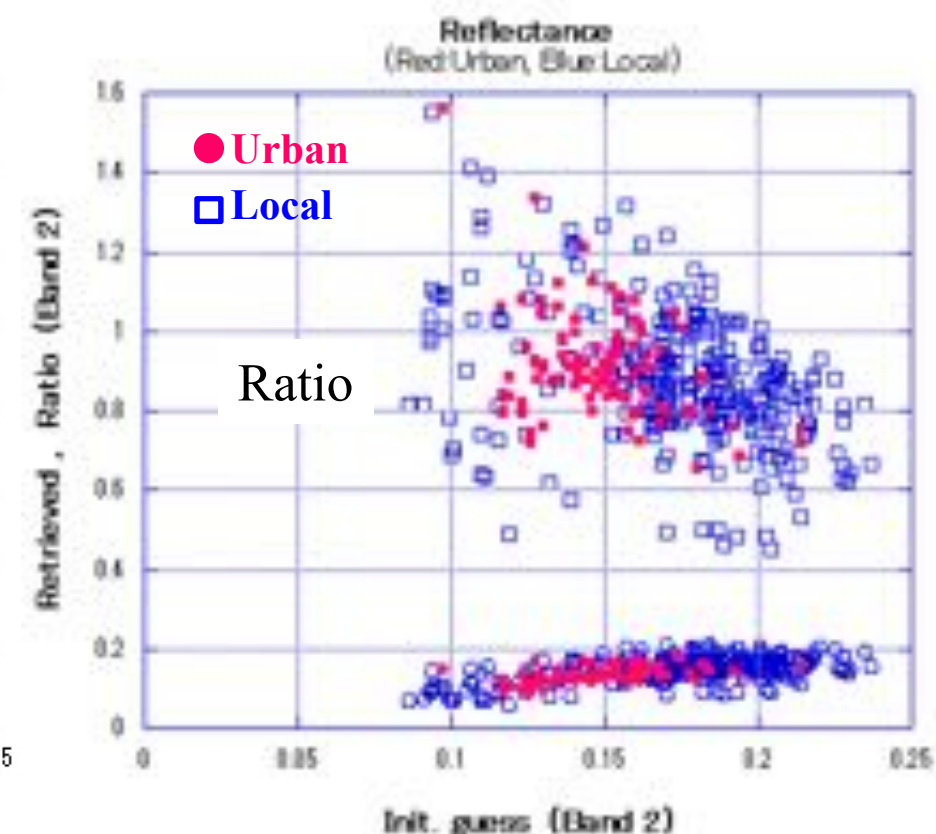
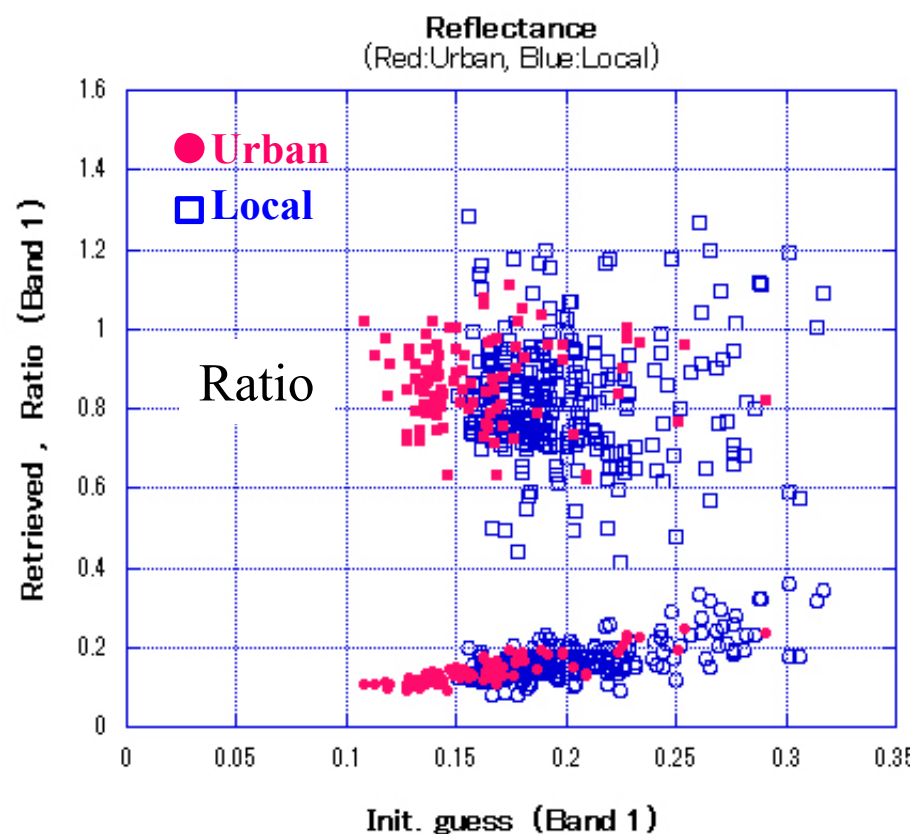
GOSAT-XCO₂ vs Wind direct./speed
2010.11~2013.3.



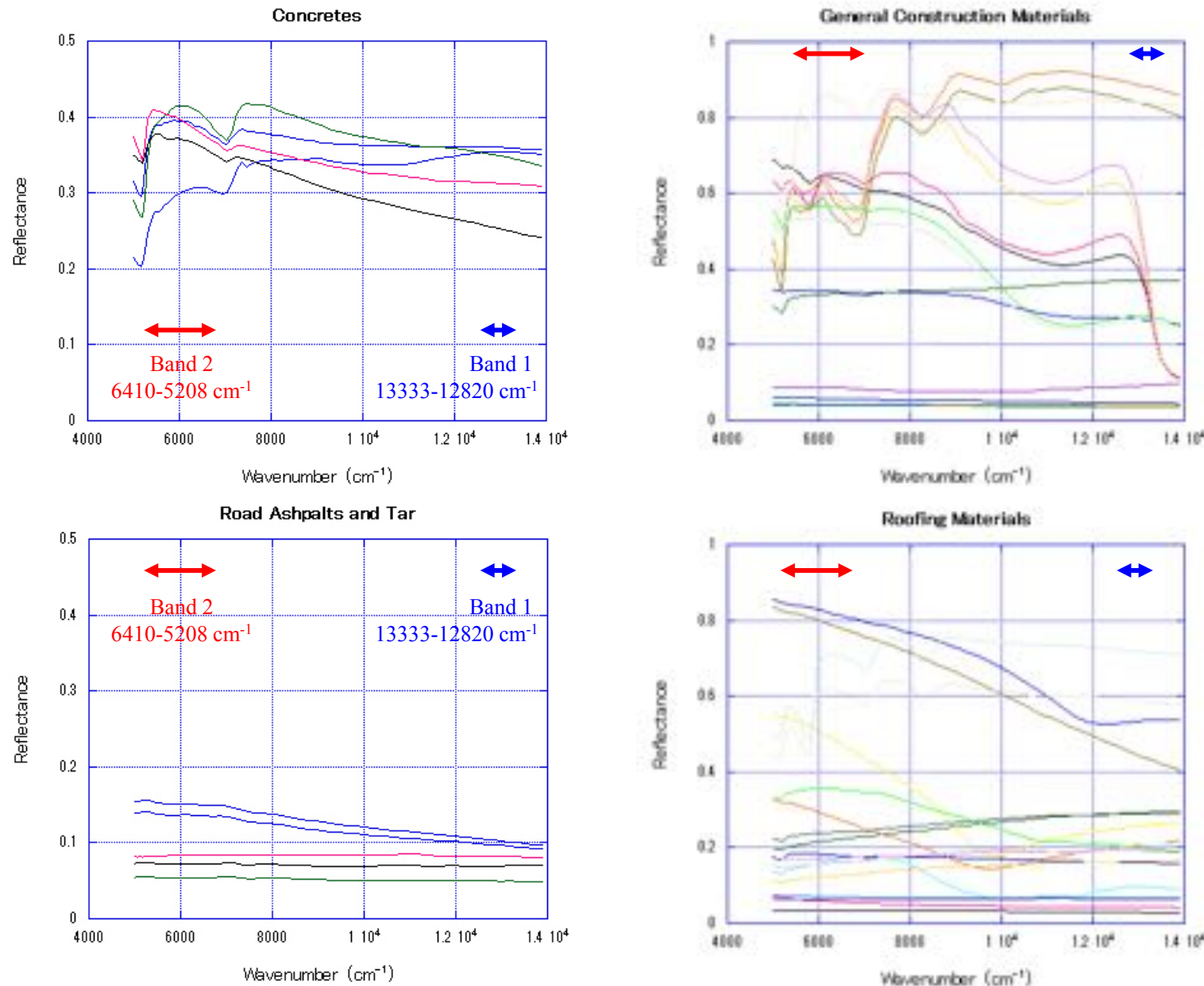
Relationship between XCO₂ and wind direction/speed

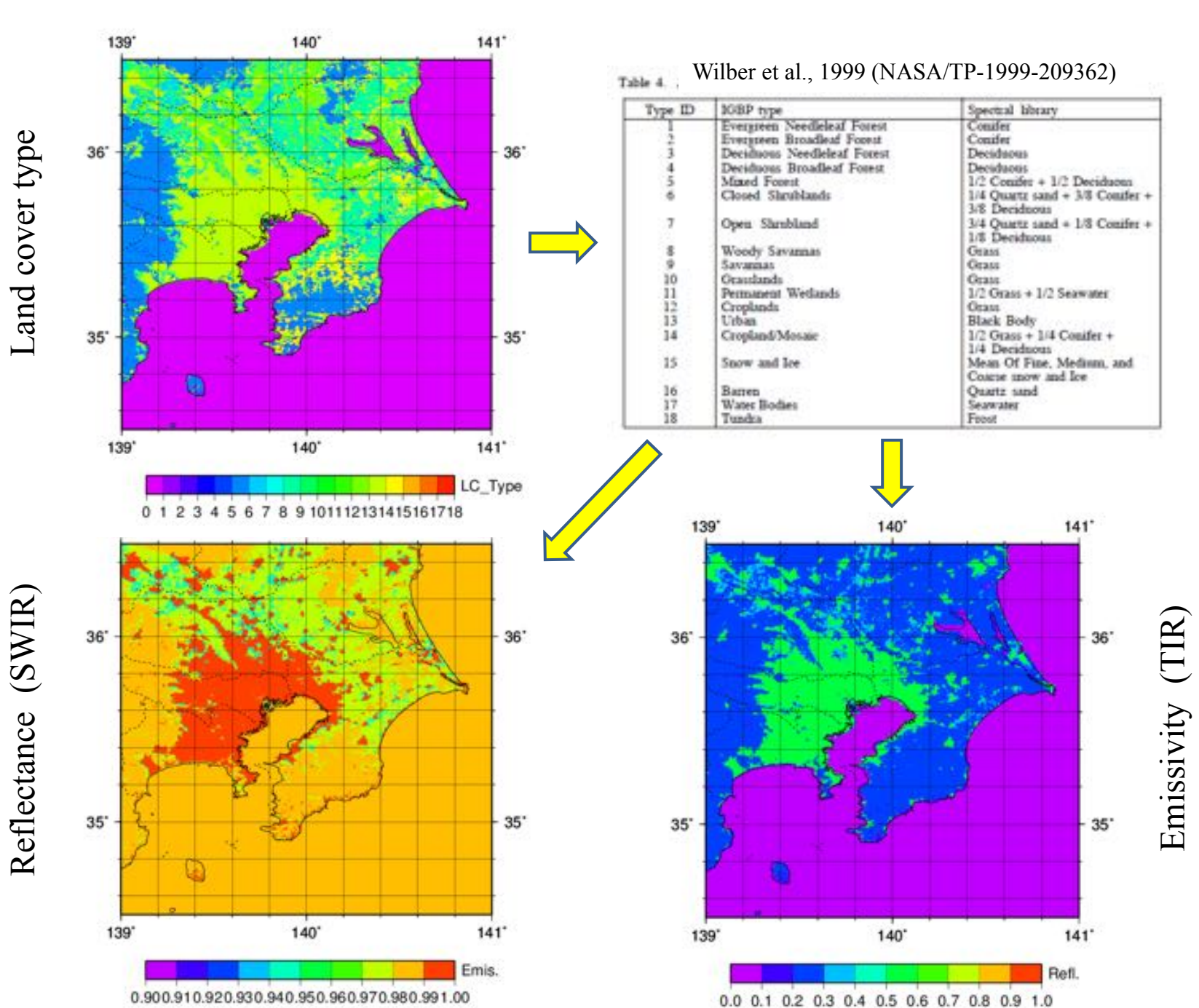


Reflectance (retrieved vs initial values)

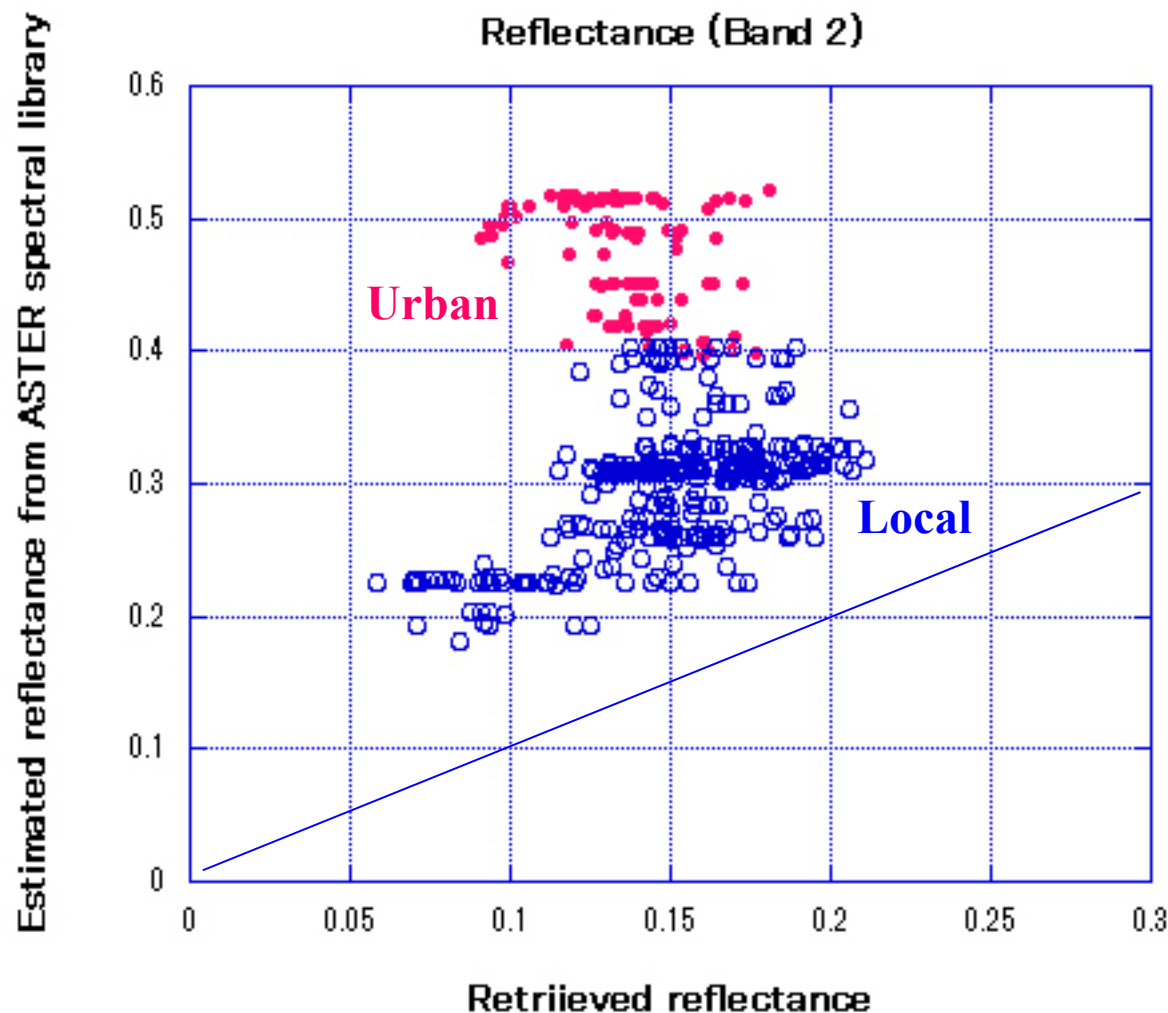


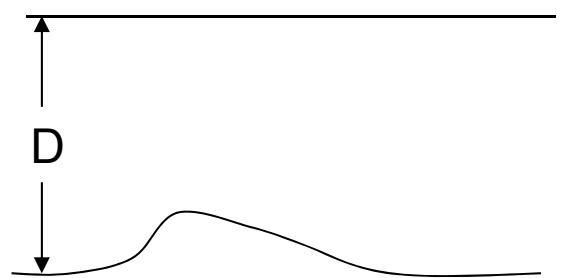
Reflectance of urban materials (ASTER spectral library)





Reflectance of urban materials (ASTER spectral library)



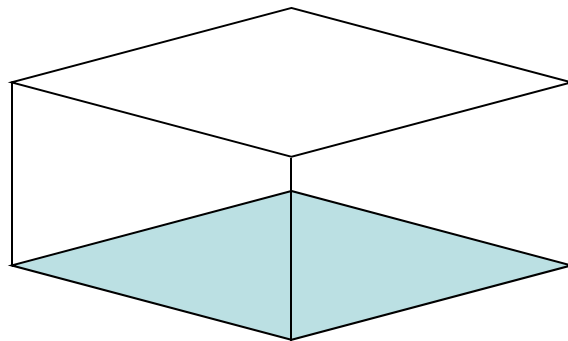


Z_T $Z_T=5500\text{m}$ (500hPa), 35 layers

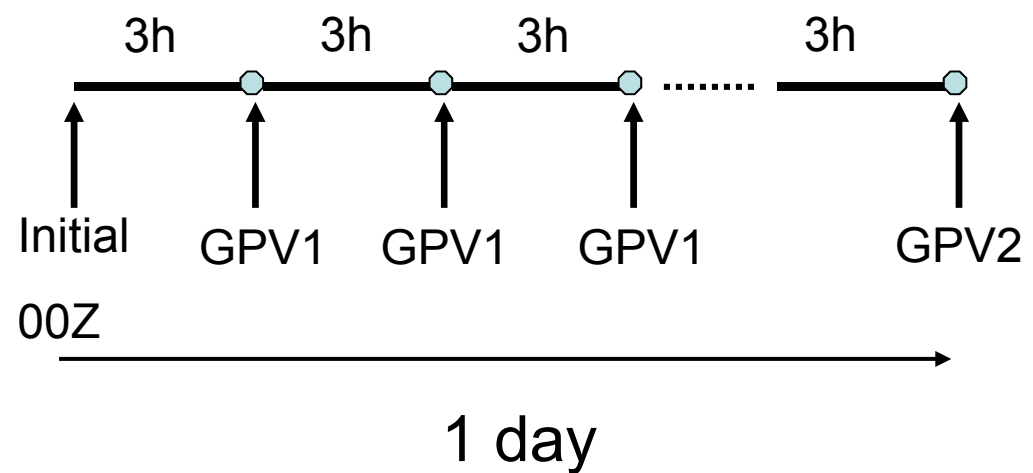
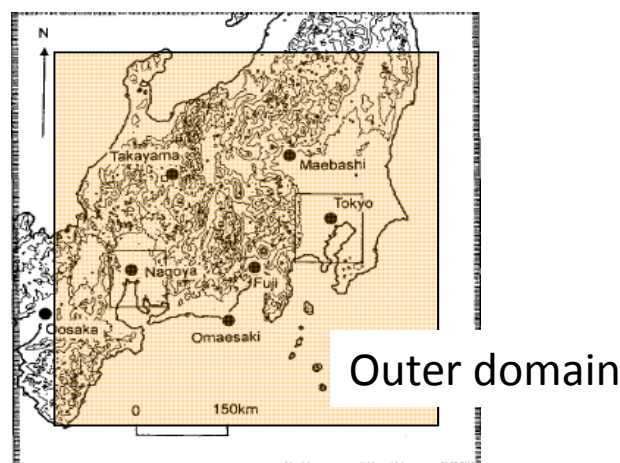
Domain: $120\text{km} \sim 600\text{km}$

Z_G Resolution: $1\text{km} \sim 10\text{km}$

Dry model



Nudging with GPV/MSM
($\text{dx}=7.5'$, $\text{dy}=5'$: for outer domain
GPV data are used every 3 hours)



Basic equations (AIST-MM)

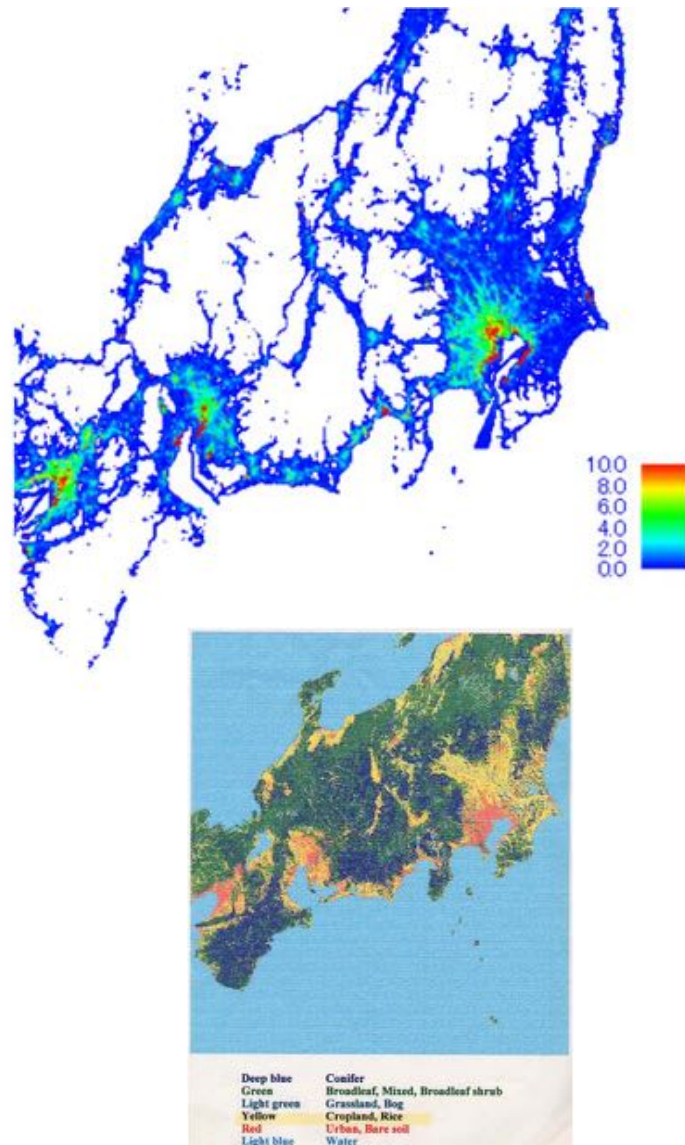
$$\begin{aligned}
 & \frac{\partial}{\partial t}(Du) + \frac{\partial}{\partial x}(Du^2) + \frac{\partial}{\partial y}(Duv) + \frac{\partial}{\partial s}(D\dot{s}u) - fDv \\
 &= -c_p\Theta D \left\{ \frac{\partial \pi}{\partial x} - (s-1)\frac{\partial D}{\partial x}\frac{g\theta}{c_p\Theta^2} \right\} \\
 &+ K_H^u D \frac{\partial^2 u}{\partial x^2} + K_H^u D \frac{\partial^2 u}{\partial y^2} + \frac{1}{D} \frac{\partial}{\partial s} \left(K_V^u \frac{\partial u}{\partial s} \right) \\
 \\
 & \frac{\partial}{\partial t}(Dv) + \frac{\partial}{\partial x}(Duv) + \frac{\partial}{\partial y}(Dv^2) + \frac{\partial}{\partial s}(D\dot{s}v) + fDu \\
 &= -c_p\Theta D \left\{ \frac{\partial \pi}{\partial y} - (s-1)\frac{\partial D}{\partial y}\frac{g\theta}{c_p\Theta^2} \right\} \\
 &+ K_H^v D \frac{\partial^2 v}{\partial x^2} + K_H^v D \frac{\partial^2 v}{\partial y^2} + \frac{1}{D} \frac{\partial}{\partial s} \left(K_V^v \frac{\partial v}{\partial s} \right) \quad (2.9)
 \end{aligned}$$

$$\frac{\partial \pi}{\partial s} = \frac{g\theta}{c_p\Theta^2} D \quad (2.10)$$

- hydrostatic model
- Terrain following coordinate system

$$\begin{aligned}
 & \frac{\partial}{\partial t}(D\theta) + \frac{\partial}{\partial x}(Du\theta) + \frac{\partial}{\partial y}(Dv\theta) + \frac{\partial}{\partial s}(D\dot{s}\theta) \\
 &= K_H^\theta D \frac{\partial^2 \theta}{\partial x^2} - K_H^\theta (s-1) \frac{\partial \theta}{\partial s} \frac{\partial^2}{\partial x^2} (\ln D) \\
 &- K_H^\theta \frac{\partial \ln D}{\partial x} (s-1) \frac{\partial}{\partial s} \frac{\partial \theta}{\partial x} \\
 &+ K_H^\theta D \frac{\partial^2 \theta}{\partial y^2} - K_H^\theta (s-1) \frac{\partial \theta}{\partial s} \frac{\partial^2}{\partial y^2} (\ln D) \\
 &- K_H^\theta \frac{\partial \ln D}{\partial y} (s-1) \frac{\partial}{\partial s} \frac{\partial \theta}{\partial y} \\
 &+ \frac{1}{D} \frac{\partial}{\partial s} \left(K_V^\theta \frac{\partial \theta}{\partial s} \right) + D \frac{\partial F}{\partial Z} \quad (2.11) \\
 \\
 & \frac{\partial}{\partial x}(Du) + \frac{\partial}{\partial y}(Dv) + \frac{\partial}{\partial s}(D\dot{s}) = 0.
 \end{aligned}$$

$$\begin{aligned}
 s &= \frac{z - z_G}{z_T - z_G}, \\
 D &= z_T - z_G \\
 \dot{s} &= \left\{ w - u \left(\frac{\partial z}{\partial x} \right) - v \left(\frac{\partial z}{\partial y} \right) \right\} \frac{\partial s}{\partial z}.
 \end{aligned}$$



Vegetation map of Japan (Bio diversity center of Japan (2000)

Anthropogenic CO₂ source: EAGrid 2000 (Kannari et al., 2007)

Natural source and sink

NEP: Net ecosystem production

GPP: Gross primary production

R: Respiration

I: Solar insolation \sim APAR

(Kondo et al., 2001)

$$NEP = \frac{bI}{1 + aI} - R \quad Q=2.5$$

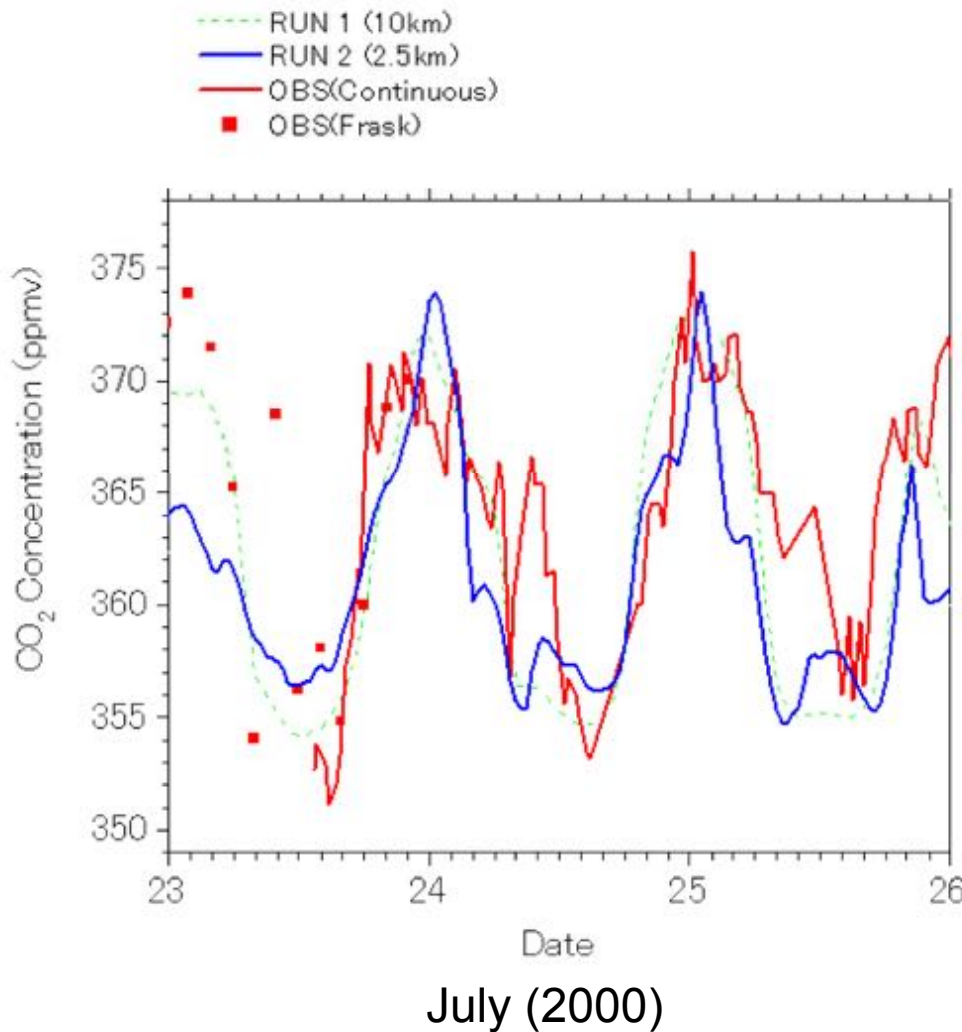
$$\frac{T-T_1}{R_I} \quad R_I=0.102$$

$$R = R_I Q^{10}$$

Table 2. *a*, *b* and *G_s* of various plant species

No.	plant species	<i>G_s</i> mm s ⁻¹	<i>a</i> J ⁻¹ sm ² × 10 ⁻⁴	<i>b</i> mgCO ₂ J ⁻¹ × 10 ⁻³
1	ever green broad leaf shrub	9.4	6.80	0.79
2	ever green conifers	20.6	6.80	1.71
3	deciduous conifers	11.4	6.80	0.95
4	deciduous broad leaf tree	20.7	6.80	1.72
5	ever green broad leaf tree	12.1	6.80	1.01
6	mixed forest	13.8	6.80	1.15
7	temperate grass land	23.0	6.80	1.92
8	bog	5.0	6.80	0.42
9	arable cropland	32.5	6.80	2.70
10	rice	25.1	6.80	2.08

Comparison at TKY (2000)



TKY flux tower (Takayama city)

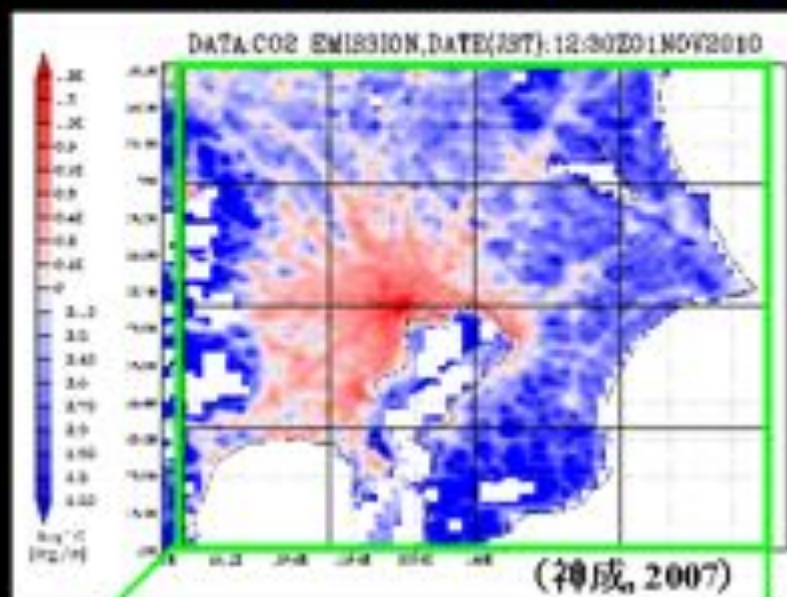
TKY

[http://asiaflux.
yonsei.ac.kr/](http://asiaflux.yonsei.ac.kr/)

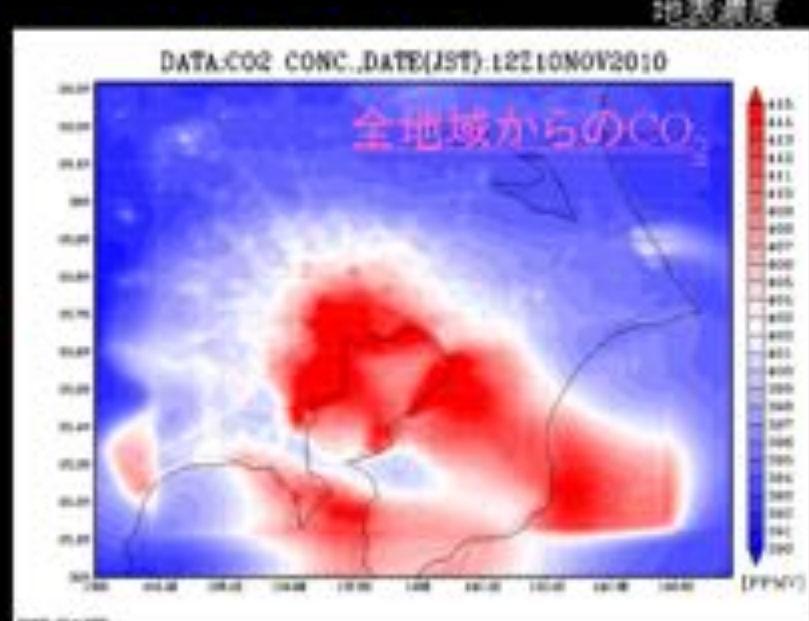


Basic calculations for synthesis inversion

全地域からの発生量



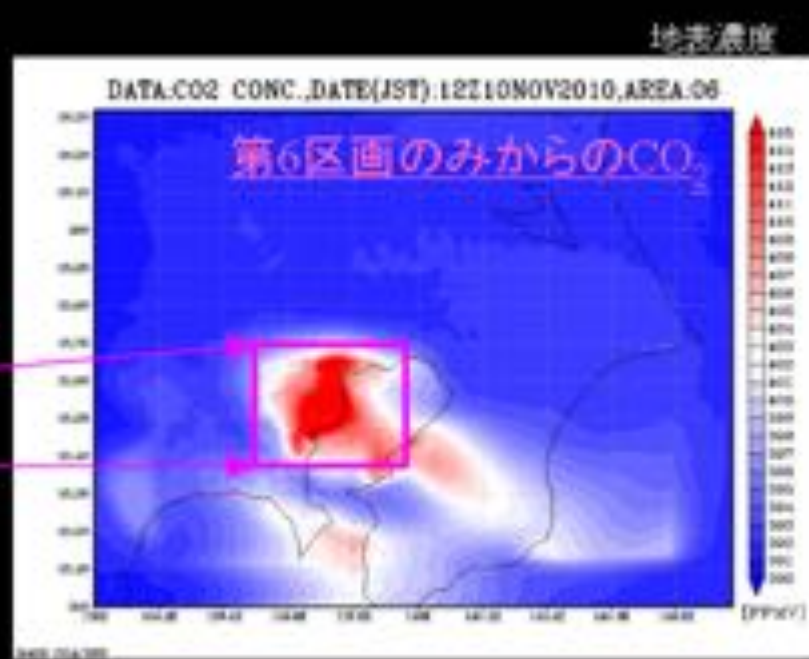
輸送計算



区画ごとの発生量



輸送計算

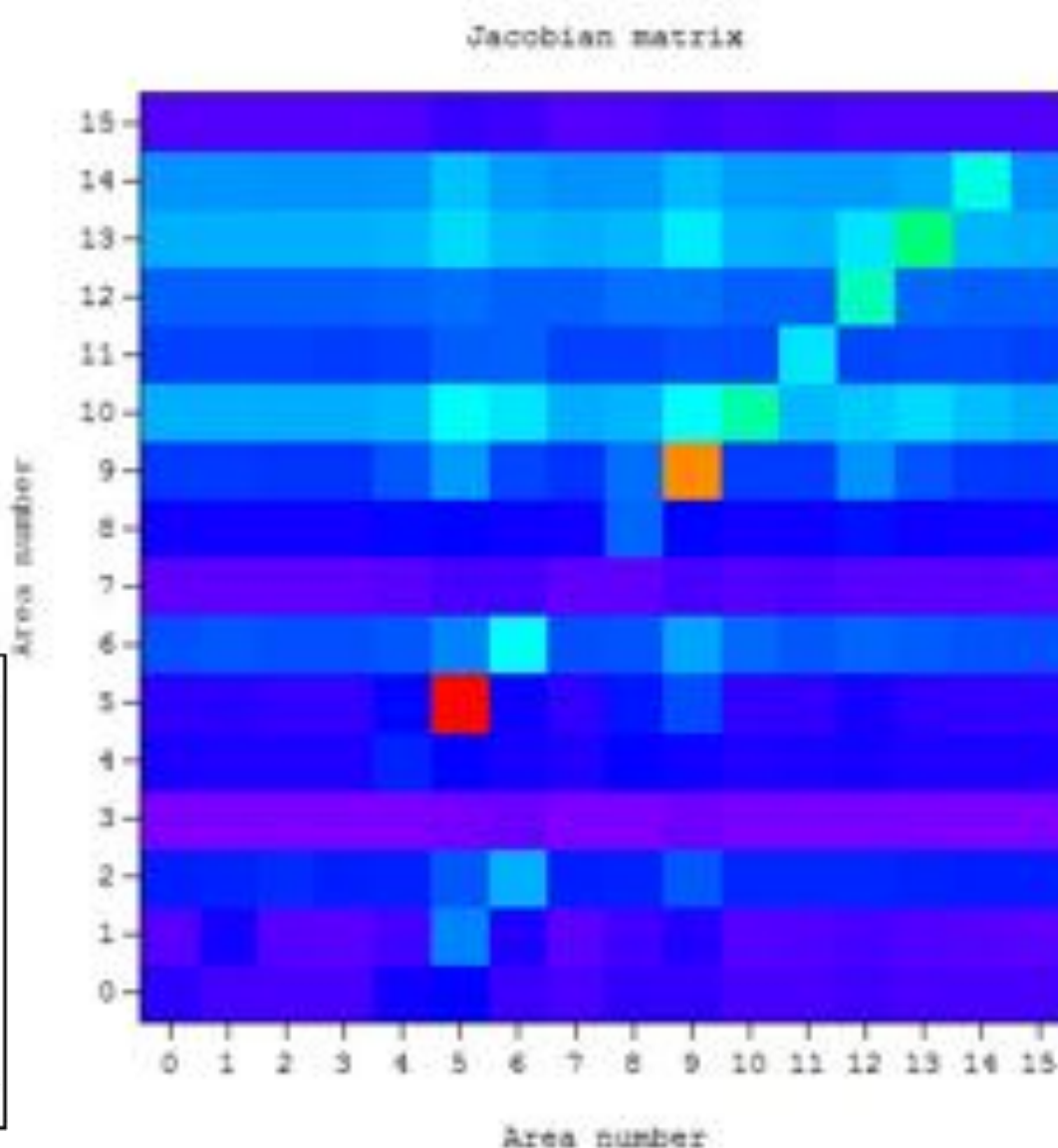
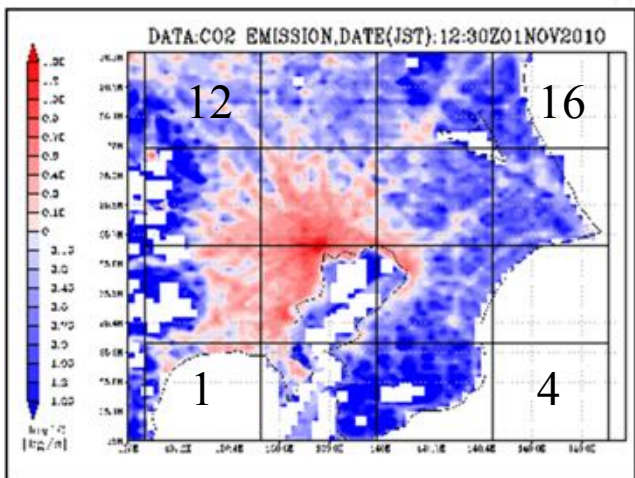




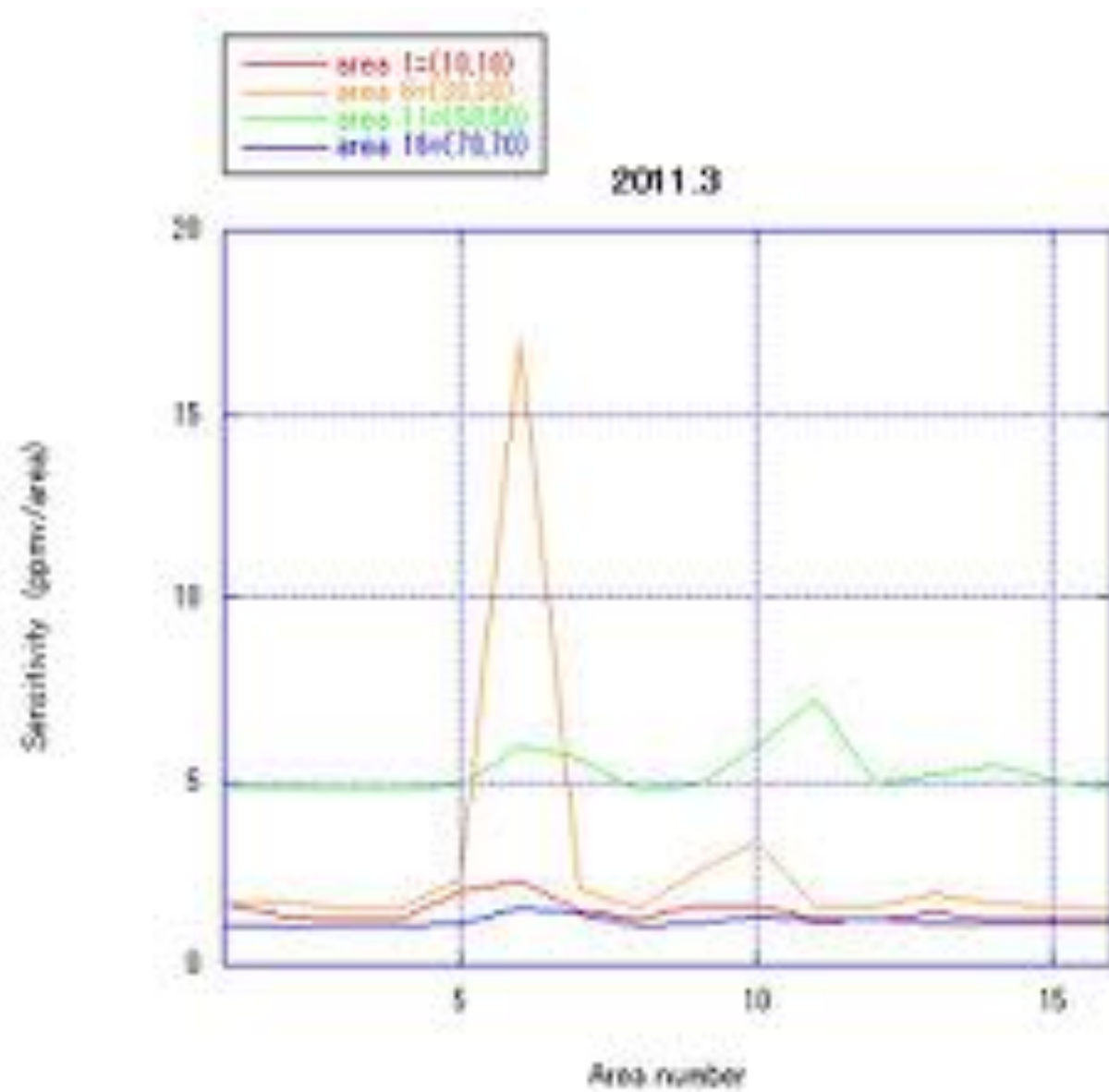
20-720x480-wmv.wmv

Example of a Jacobean matrix used for synthesis inversion analysis

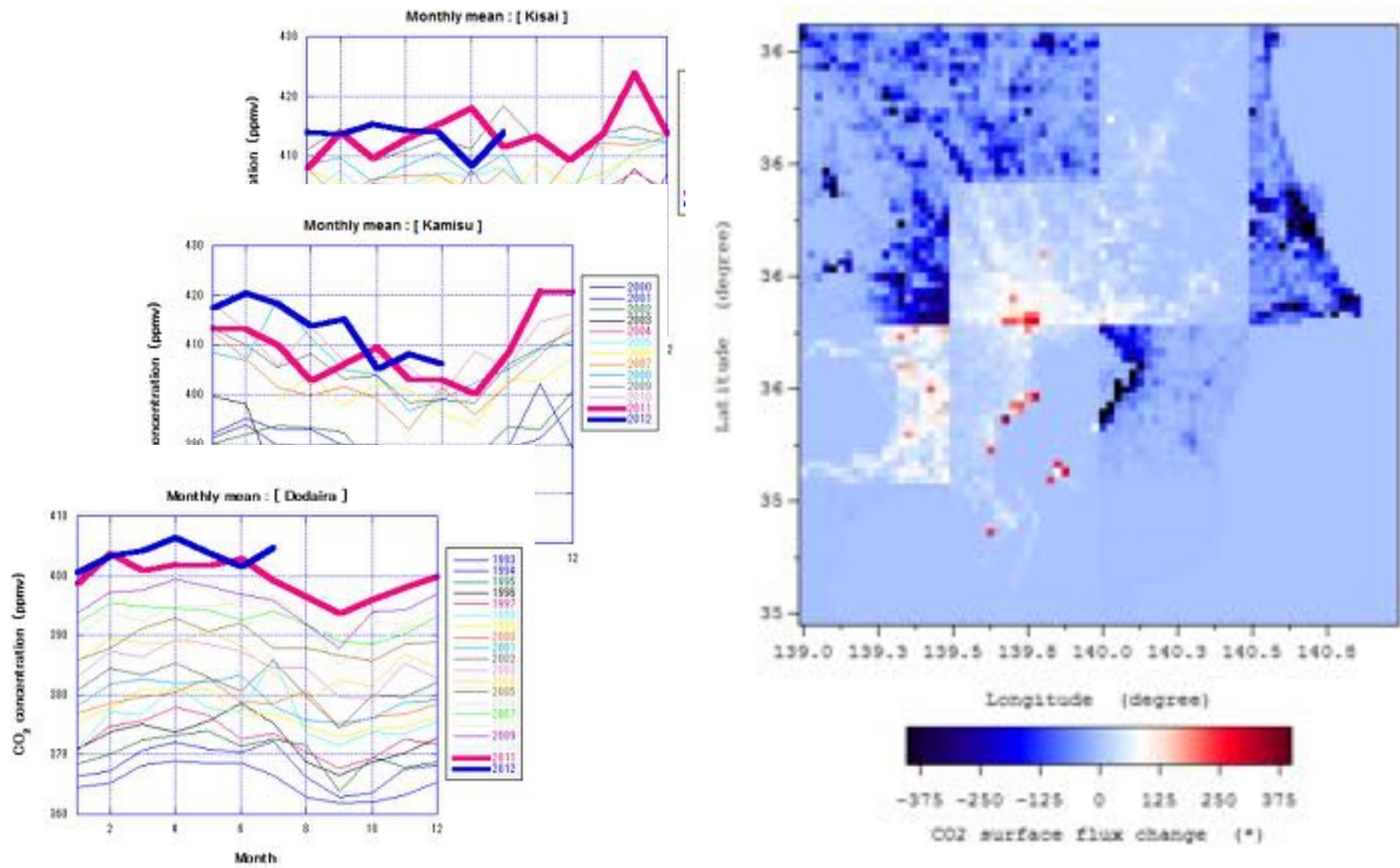
- case for 2011.3
- only surf. data were used
- all hourly data were used
- assumed that there is one observation site in each block area
- observational error is infinite



Example of horizontal resolution functions

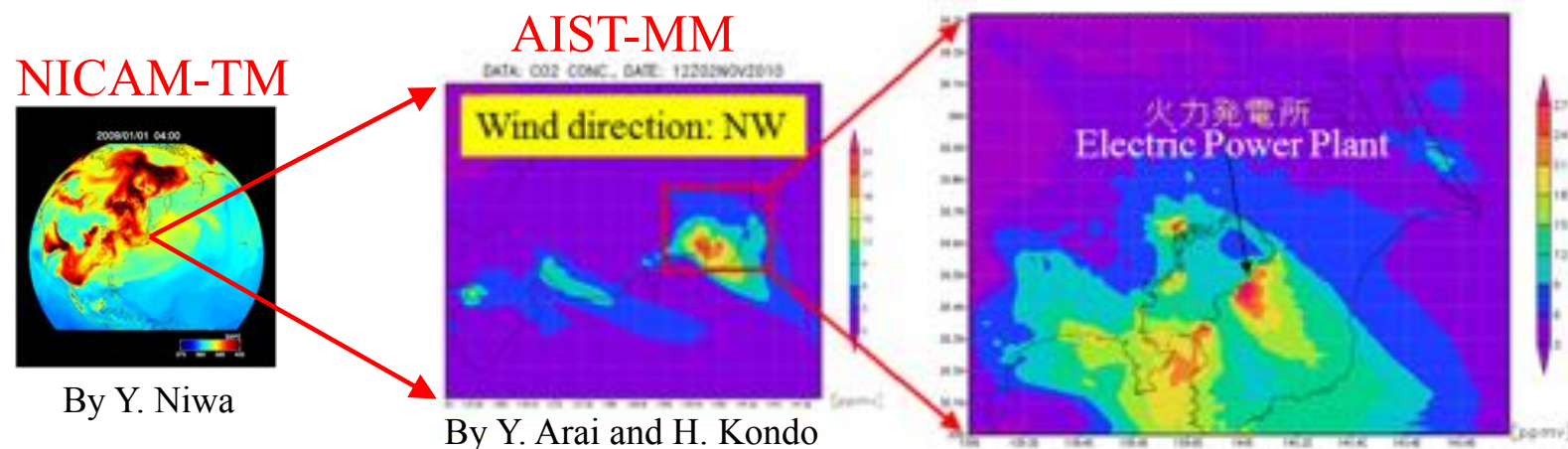


Result from synthesis inversion analysis using AIST-MM (monthly average for 2011.3; only surface data were used)

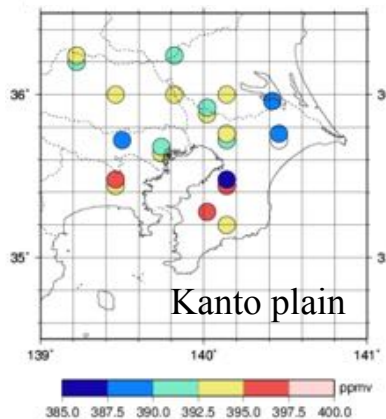


Global → Regional (urban area)

Max. resolution = 1km x 1km

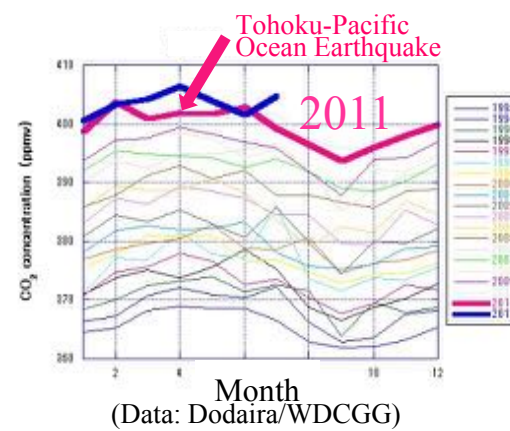


GOSAT
targeting observation



+

Ground-based
in situ measurements



Changes
in emission strength



Inversion
(synthesis)

